Diamond-anvil cell for radial x-ray diffraction

2006 J. Phys.: Condens. Matter 18 S1083

(http://iopscience.iop.org/0953-8984/18/25/S15)

INSTITUTE OF PHYSICS PUBLISHING JOURNAL OF PHYSICS: CONDENSED MATTER

J. Phys.: Condens. Matter **18** (2006) S1083–S1090 doi:10.1088/0953-8984/18/25/S15

Diamond-anvil cell for radial x-ray diffraction

G N Chesnut, D Schiferl, B D Streetman and W W Anderson

Los Alamos National Laboratory, Los Alamos, NM 87545, USA

Received 14 January 2006, in final form 20 March 2006
Published 8 June 2006
Online at stacks.iop.org/JPhysCM/18/S1083

Abstract

We have designed a new diamond-anvil cell capable of radial x-ray diffraction to pressures of a few hundred GPa. The diffraction geometry allows access to multiple angles of Ψ, which is the angle between each reciprocal lattice vector $\mathbf{g}(\boldsymbol{hkl})$ and the compression axis of the cell. At the 'magic angle', $\Psi \approx 54.7°$, the effects of deviatoric stresses on the interplanar spacings, $d(hkl)$, are significantly reduced. Because the systematic errors, which are different for each $d(hkl)$, are significantly reduced, the crystal structures and the derived equations of state can be determined reliably. At other values of Ψ, the effects of deviatoric stresses on the diffraction pattern could eventually be used to determine elastic constants.

(Some figures in this article are in colour only in the electronic version)

1. Introduction

High-pressure and high-temperature conditions are achieved by static and dynamic techniques. The focus of this discussion will be on a specific static technique. Static high-pressure experiments provide detailed information about phase-transition boundaries, crystal structures of high-pressure phases and equations of state [1–4]. Since the invention of diamond-anvil cells (DACs) in 1959 [5, 6], this information has typically been collected from *in situ* x-ray powder diffraction from samples in these cells. Unfortunately, controversies over the high-pressure crystal structures, especially those of low-symmetry phases, date back nearly as far as diamond-anvil cells. In extreme cases, the volume changes at phase boundaries for the same material under nominally identical conditions have differed from 9.8% to 19% [7–9].

A major problem, which was recognized very early on, is the effect of non-hydrostatic pressures on the diffraction patterns [10][1] and [11]. Under non-hydrostatic conditions, there are two independent sources of error: large pressure gradients, and systematic shifts in the $d(hkl)$, due to deviatoric stress effects that are different for each $d(hkl)$. Both of these problems contributed to the difficulties of interpreting early high-pressure diffraction patterns.

[1] Jamieson collected hundreds diffraction patterns that he did not publish because the errors in the calculated cell parameters were larger than he could account for on the basis of experimental uncertainties. When the Singh and Kennedy [11] results were published, he recognized immediately that they had identified the principal problem.

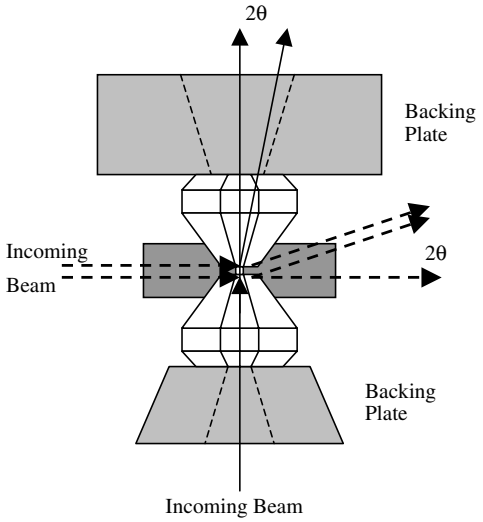

Figure 1. The diamond interface and sample region of the DAC. The solid lines represent axial diffraction and the heavy dashed lines represent radial diffraction. The light dashed lines represent openings in the backing plates.

Modern diffraction experiments with intense synchrotron and laboratory radiation sources allow collimation of the x-ray beams to a few microns so that only a small pressure variation is sampled. However, deviatoric stresses cause subtle shifts in the diffraction patterns with dramatic consequences and therefore cannot be ignored. They are currently the most important source of error for equations of state of materials with low-symmetry structures, primarily because the incorrect $d(hkl)$ may lead to incorrect crystal structures. Moreover, the errors due to deviatoric stresses increase as the pressure increases.

The invention of the gasketed diamond-anvil cell in 1964 allowed fluids to be loaded either as samples or as hydrostatic pressure media [12]. Common pressure media include methanol–ethanol mixtures, nitrogen, argon, and helium. At room temperature, all known pressure media freeze below about 12 GPa, far below the 100–200 GPa that can be routinely generated in diamond-anvil cells [13]. As long as the pressure medium has a lower shear strength than the sample, the pressure can be considered as quasi-hydrostatic. Remarkably, helium is nearly hydrostatic up to approximately 100 GPa, although it is somewhat difficult to use. Helium is challenging to load into a DAC. Moreover, because it has so little shear strength, the helium pressure medium does not help the gasket support pressure; and the gasket must therefore be thinner to maximize friction. This in turn makes it more likely that the sample will bridge the diamonds and therefore be subject to deviatoric stresses. Thus, in practice, many experiments will be done under non-hydrostatic conditions, and it is important to design them with this fact in mind.

2. X-ray diffraction under non-hydrostatic pressures in diamond-anvil cells

The configuration of a DAC is shown in figure 1. Two opposed diamond anvils are supported by carbide or steel backing plates. A metal gasket is placed between the diamonds to contain the sample. The force of several hundred GPa on the diamonds can be applied by a variety of mechanisms.

The DAC can be used in two possible geometries with respect to the incoming x-ray beam. The most common experimental geometry, axial diffraction, is illustrated in figure 1 by the solid lines. The other geometry is known as radial diffraction and is illustrated by the heavy dashed lines. θ is the Bragg angle in the axial and radial geometry. The purpose for using the two different geometries will be discussed in detail below. However, it should be pointed out that there are some issues in attempting radial diffraction in most DACs. First, DACs are constructed of metal with few openings for incoming and outgoing beams [14]. Second, common gasket materials, such as steel or Inconel, are practically opaque to x-rays.

The sample experiences stress in the axial direction from the diamonds and experiences stress in the radial direction from the gasket material. At the centre, the stress state of the sample is experiencing compression in the axial direction and tension in the radial direction [15, 16]. The deviatoric stress causes the measured interplanar spacing, $d_{\mathrm{m}}(hkl)$, to vary depending on the angle Ψ, which is the angle between the reciprocal lattice vector, $\boldsymbol{g}(\boldsymbol{hkl})$, and the compression axis. This leads to errors in equation of state (EOS) parameters such as pressure and volume. Most importantly, incorrect $d(hkl)$ may lead to incorrect crystal structure determinations, a problem that is worse for low-symmetry structures.

Recent studies have alluded to a new way of removing deviatoric stress effects from measurements or to use them to determine elastic constants for high-pressure phases. Singh *et al* [17] developed the equations governing lattice strains in non-hydrostatic environments. These equations depend on the degree of deviatoric stress and the properties of the sample. The equation of particular interest is

$$d_{\mathrm{m}}(hkl) = d_{\mathrm{p}}(hkl)[1 + (1 - 3\cos^2\Psi)Q(hkl)], \tag{1}$$

where $d_{\mathrm{m}}(hkl)$ is the measured interplanar spacing, $d_{\mathrm{p}}(hkl)$ is the hydrostatic interplanar spacing, and $Q(hkl)$ is a complicated function of the elastic constants of the material at high pressure. Ψ is the angle between $\boldsymbol{g}(\boldsymbol{hkl})$ and the compression axis. Equation (1) assumes that the sample has a finite yield strength and that the sample is pressurized by a uniaxial load. Unfortunately, equation (1) is practically impossible to solve for orthorhombic and lower-symmetry structures. However, a particularly simple solution occurs when $1 - 3\cos^2\Psi = 0$. For this to be true, $\Psi \approx 54.74°$ (the magic angle), and $d_{\mathrm{m}}(hkl) = d_{\mathrm{p}}(hkl)$. By choosing the magic angle [18], the effects of the deviatoric stresses (although not the stresses themselves) have been removed from the data. While this analysis is strictly true only at the very centre of the sample, Singh and co-workers [17] have demonstrated that the analysis for this radial diffraction technique is a good approximation with a sample disc 10 μm thick and 25 μm diameter and an x-ray beam of 5 μm diameter. However, Singh *et al*'s equations should be applied carefully to ensure that the necessary assumptions have been met [19, 20].

Radial x-ray diffraction has become increasingly popular in the last several years [16, 21–25]. There are few DACs that are capable of radial diffraction. Some of the early designs have disadvantages such as beryllium backing plates, which lead to a pressure limit [26]. We have designed a new radial diffraction DAC, as shown in figures 2 and 3, with a large side aperture that can access the magic angle and all angles between $\Psi = 0°$ and 90°. The x-ray beam enters the DAC through the large D-shaped opening (see figure 3), and diffracts out of the opposite side providing a diffraction angle, 2θ, up to approximately 45°. The magic-angle DAC is modelled after a DAC used by Dr Yogesh Vohra that is capable of pressures over 400 GPa. The DAC is a piston-cylinder type cell made of stainless steel. The driving mechanism is a finely threaded bolt (40 threads/inch), which provides a fine control of the pressure and a parallel diamond interface during compression. The diamond backing plates are made of A-2 tool steel and are heat-treated to a Rockwell hardness (RH) of 55. The bottom plate has an x–y positioning control, and the top plate has a tilt control which leads to an accurate

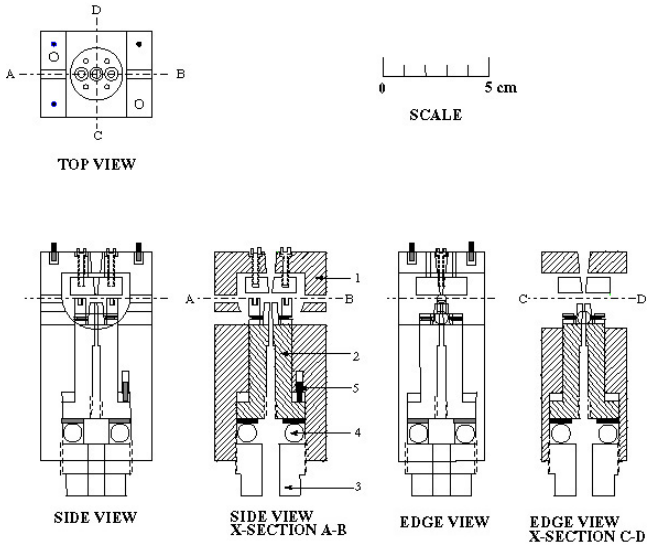

Figure 2. Magic-angle diamond-anvil cell. The diamond anvils are not shown because they are too small to show up clearly. They are located where the dashed lines A–B and C–D meet. The cell is presented in three orthogonal views as well as two cross-sections. The key feature is an open yoke (1) for maximum x-ray access. Pressure is applied to the piston (2) by turning a nut (3), which applies the load to a ball-bearing race (4) to minimize torque on the piston. The piston alignment is maintained by a pin (5). The compression axis is along the long cell axis.

Figure 3. Magic-angle diamond-anvil cell.

and stable alignment of the diamonds. A gasket material that allows the transmission of x-rays must be used for the radial diffraction technique. The best material known thus far for achieving pressures of hundreds of GPa is beryllium (Be) metal [27]. Due to its low atomic number and relatively high strength, it provides the necessary support with minimal x-ray absorption[2]. The Be gasket used in this cell is approximately 3 mm × 15 mm × 0.25 mm. The diffraction rings from the Be gasket interfere with the sample rings; however, this can be greatly reduced by

[2] Mass absorption coefficients, μ/ρ (cm^2 g^{-1}), for principal components in common gaskets at $\lambda = 0.711$ Å: Be—0.245, Fe—37.74, Re—98.74, Rh—23.05, Ni—47.24.

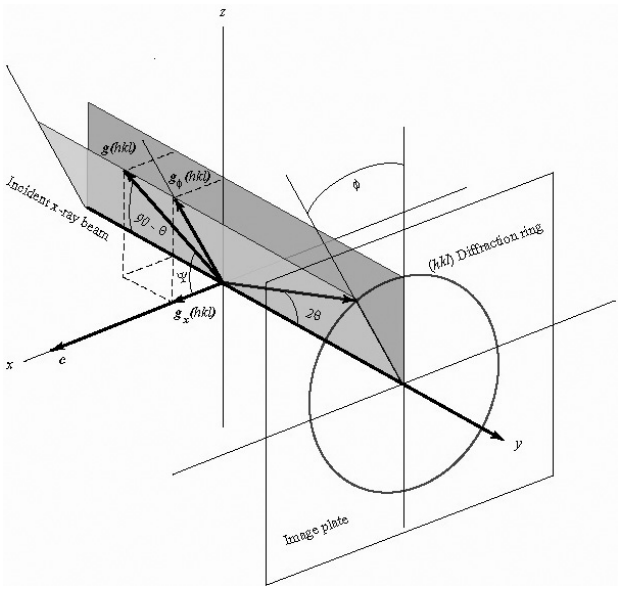

Figure 4. A diagram of the radial diffraction technique that relates the angle Ψ, diffracting planes, and corresponding reflection points on the image plate. The angle Ψ is the angle between the compression axis, $\boldsymbol{c}$, and the reciprocal lattice vector, $\boldsymbol{g(hkl)}$.

rotating the cell a few degrees so that the x-ray beam goes through much less Be. Another gasket material is amorphous boron, which has been tested up to 65 GPa [28, 29].

The new cell provides access to the magic angle as illustrated in figures 1 and 4. The compression axis of the magic-angle DAC is given by $\boldsymbol{c}$. The direction of $\boldsymbol{c}$ becomes important when calculating Ψ, as will be discussed later. The reciprocal lattice vector, the projection of the reciprocal lattice vector along the x-axis, and the projection of the reciprocal lattice vector along the ϕ-direction are given by $\boldsymbol{g(hkl)}$, $\boldsymbol{g_x(hkl)}$, and $\boldsymbol{g_\phi(hkl)}$, respectively. It should be noted that the angle between ϕ and Ψ on the image plate is relatively small, but it should be carefully calculated, as will be discussed.

By using the magic-angle DAC along with an area detector, such as a CCD or an image plate, one can collect a vast amount of information from each set of ring patterns. Interpreting the three-dimensional diffraction pattern that is projected onto a two-dimensional screen takes more effort with the radial diffraction technique than the axial diffraction technique. In the axial geometry all the points on a particular ring represent the same value of Ψ, which provides minimal information with respect to the stress–strain of the sample. However, in the radial geometry each point of a particular ring represents a different value of Ψ in each quadrant, which is illustrated in figure 4. By using spherical coordinates and the diffraction geometries of planes, the Ψ values for each point on the two-dimensional screen can be mapped out. The compression axis vector, $\boldsymbol{c}$, and the reciprocal lattice vector, $\boldsymbol{g(hkl)}$, are

$$\boldsymbol{c} = \cos\phi_c \cos\theta_c \hat{\imath} - \cos\phi_c \sin\theta_c \hat{\jmath} + \sin\phi_c \kappa \tag{2}$$

$$\boldsymbol{g(hkl)} = \cos\phi_g \cos\theta_g \hat{\imath} - \cos\phi_g \sin\theta_g \hat{\jmath} + \sin\phi_g \kappa. \tag{3}$$

By taking the dot product of $\boldsymbol{c}$ and $\boldsymbol{g(hkl)}$, Ψ can be related to ϕ_g, θ_g, and θ_c.

$$\boldsymbol{c} * \boldsymbol{g(hkl)} = cg \cos\Psi \qquad (\text{for } 0 \leqslant \Psi \leqslant \pi) \tag{4}$$

$$\cos\Psi = \cos\phi_g \cos(\theta_g - \theta_c) \tag{5}$$

$$\cos\phi_g = \cos\Psi / \cos(\theta_g - \theta_c). \tag{6}$$

This relationship allows one to determine Ψ for any point on the area detector. Placing the compression axis into the x–y plane and assuming the vector lengths to be unity have simplified this derivation. Also, $\boldsymbol{c}$ should be taken in the positive x direction if $\boldsymbol{g}(\boldsymbol{hkl})$ is in the positive x direction, or $\boldsymbol{c}$ should be taken in the negative x direction if $\boldsymbol{g}(\boldsymbol{hkl})$ is in the negative x direction, to avoid violating the rule in equation (4). It should also be noted that as Ψ approaches 0 the number of diffraction points becomes limited. A practical limit at which to measure Ψ is about 10°.

The radial diffraction technique provides $d_{\mathrm{m}}(hkl)$ at the magic angle, $\Psi \approx 54.74°$, which produces accurate EOS parameters. By taking advantage of the $d_{\mathrm{m}}(hkl)$ for each Ψ value and Singh *et al*'s [17] equations, elastic constants from relatively high symmetry structures could eventually be determined [21, 30]. When calculating elastic moduli it is important to address the effects of plasticity [31, 32]. The accuracy of the elastic constants may not be very good; however, this is the only technique for making such measurements at pressures of hundreds of GPa.

Another feature of this technique is that the four quadrants of the area detector have a relative symmetry, which provides four diffraction patterns ($d_{\mathrm{m}}(hkl)$ versus intensity) at each angle of Ψ. By comparing the $d_{\mathrm{m}}(hkl)$ of each of the four quadrants, the presence of pressure gradients and/or inhomogeneities of the sample can be determined. More importantly, by comparing the $d_{\mathrm{m}}(hkl)$ of each of the four quadrants, the precision of the measured pressure and volume can be improved by statistics for any angle of Ψ including the magic angle. Using these techniques, the effects of deviatoric stress have been recently demonstrated [17, 22], and warrant further examination, especially on low-symmetry structures.

3. Preliminary results and discussion

Recent experiments have helped to further demonstrate the importance of the radial diffraction technique. First, a polycrystalline cerium sample was loaded into a magic-angle DAC and compressed to a pressure of 47 GPa. The radial x-ray diffraction pattern at the maximum pressure was analysed using the equations defined in the previous section. $d_{\mathrm{m}}(101)$ of the body-centred tetragonal phase in cerium was plotted with respect to Ψ as shown in figure 5.

The deviatoric stress created a systematic error in $d(101)$ with maximum error of 1%. This relatively small deviation in $d(101)$ produces a maximum error in the volume (V/V_0) of 3%. The error in $d(101)$ is calculated as the difference of $d(101)$ between $\Psi \approx 0°$ and 90°, and the error in V/V_0 is calculated in the same manner. This clearly demonstrates that small systematic errors from deviatoric stress perpetuate into significant errors in the equation of state parameters. However, lower-symmetry structures with closely spaced $d(hkl)$ present further complications beyond systematic errors.

Another experiment performed on zirconium at 19 GPa demonstrates this as shown in figure 6. The portion of the diffraction ring at the magic angle seems to have higher resolution than other parts of the same ring with respect to $d(101)$ and $d(110)$. At $\Psi = 90°$, the ring is noticeably broader and fuzzier than around $\Psi = 54.7°$, which is the only region where the splitting between the rings is apparent, as can be seen at point (a) in figure 6. Presumably, resolution is higher because the range of deviatoric stress effects across the finite sample dimensions is especially small for crystallites diffracting under magic-angle conditions.

The results of this study and others in the past several years demonstrate that radial x-ray diffraction provides a wealth of information. X-ray diffraction data can be collected at the magic angle where the deviatoric stress effects cancel, providing hydrostatic results and avoiding the complicated strain equations. However, careful analysis should be performed when using Singh *et al*'s equations. Elastic constants from relatively high-symmetry structures

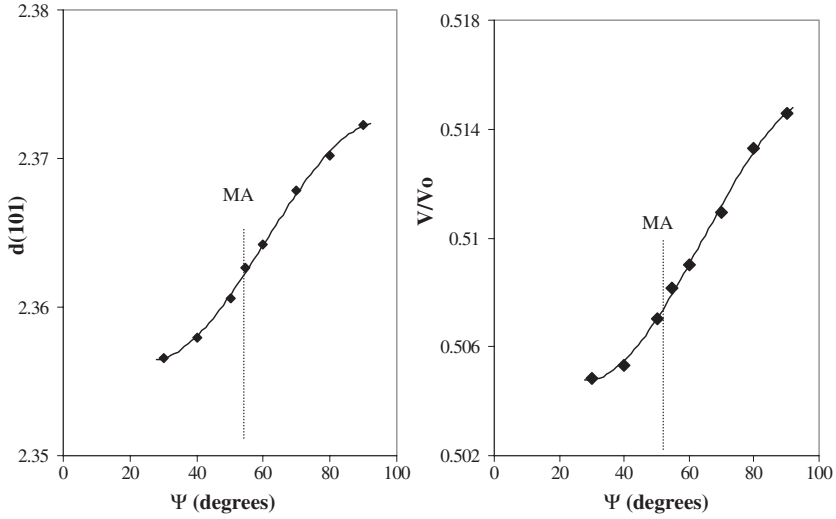

Figure 5. Cerium at 47 GPa in the magic-angle DAC. Ψ versus $d(101)$ shows a maximum error of 1% in $d(101)$ with respect to varying Ψ. Ψ versus V/V_0 shows a maximum error of 3% in V/V_0 with respect to varying Ψ. MA is the magic angle.

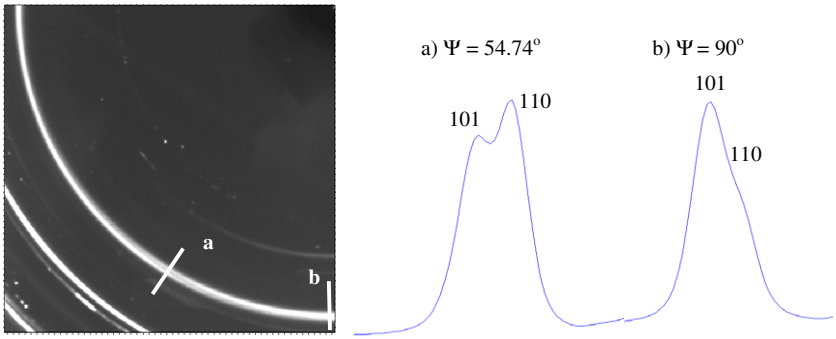

Figure 6. On the left is part of a diffraction pattern of zirconium at 19 GPa. Point a shows the resolution between $d(101)$ and $d(110)$ at the magic angle. Point (b) shows the resolution between the same two peaks at $\Psi = 90°$, which approximately corresponds to axial diffraction results.

cannot be determined using existing techniques; however, by taking advantage of the deviatoric stresses at pressure this could eventually be possible.

Acknowledgment

This work was, in part, supported by the US DOE under contract No W-7405-ENG-36.

References

[1] Jayaraman A 1983 *Rev. Mod. Phys.* **55** 65
[2] Jayaraman A 1986 *Rev. Sci. Instrum.* **57** 1013
[3] Hazen R M and Downs R T 2000 *High-Temperature and High-Pressure Crystal Chemistry* (Washington: Mineralogical Society of America)
[4] Hemley R J and Ashcroft N W 1998 *Phys. Today* **51** 26

[5] Jamieson J C, Lawson A W and Nachtrieb N D 1959 *Rev. Sci. Instrum.* **30** 1016
[6] Weir C E, Lippincott E R, Van Valkenburg A and Bunting E N 1959 *J. Res. Natl Bur. Stand.* A **63** 55
[7] Mao H K, Hazon R M, Bell P M and Wittig J 1981 *J. Appl. Phys.* **52** 4572
[8] Smith G S and Akella J 1982 *J. Appl. Phys.* **53** 9212
[9] Chesnut G N and Vohra Y K 2000 *Phys. Rev.* B **62** 2965
[10] Jamieson J C 1971–1975 private communications to DS
[11] Singh A K and Kennedy G C 1974 *J. Appl. Phys.* **45** 4686
[12] Whatley L S, Lippincott E R, Van Valkenburg A and Weir C E 1964 *Science* **144** 968
[13] Piermarini G J, Block S and Barnett J D 1973 *J. Appl. Phys.* **44** 5377
[14] Jayaraman A 1983 *Rev. Mod. Phys.* **55** 65
[15] Singh A K and Balasingh C 1977 *J. Appl. Phys.* **48** 5338
[16] Meng Y and Weidner D J 1993 *Geophys. Res. Lett.* **20** 1147
[17] Singh A K, Balasingh C, Mao H K, Hemley R J and Shu J 1998 *J. Appl. Phys.* **83** 7567
[18] Chesnut G N, Streetman B D, Schiferl D, Anderson W W, Nicol M and Meng Y 2004 Shock compression of cond. matt.-2003 *Conf. Proc. APS Topical Group on SCCM* ed M D Furnish, Y M Gupta and J W Forbes (New York: AIP) p 37 (Pt. 1)
[19] Matthies S, Priesmeyer H G and Daymond M R 2001 *J. Appl. Crystallogr.* **34** 585
[20] Matthies S, Merkel S, Wenk H R, Hemley R J and Mao H K 2001 *Earth Planet. Sci. Lett.* **194** 201
[21] Duffy T S, Shen G, Shu J, Mao H K, Hemley R S and Singh A K 1999 *J. Appl. Phys.* **86** 6729
[22] Shieh S R, Duffy T S and Li B 2002 *Phys. Rev. Lett.* **89** 255507
[23] Merkel S, Wenk H K, Shu J, Shen G, Gillet P, Mao H K and Hemley R J 2002 *J. Geophys. Res.* B **107** 2271
[24] Merkel S, Jephcoat A P, Shu J, Mao H K, Gillet P and Hemley R J 2002 *Phys. Chem. Minerals* **29** 1
[25] Kavner A and Duffy T S 2003 *Phys. Rev.* B **68** 144101
[26] Schiferl D, Jamieson J C and Lenko J E 1978 *Rev. Sci. Instrum.* **49** 359
[27] Hemley R J, Mao H K, Shen G, Badro J, Gillet P, Hanfland M and Hausermann D 1997 *Science* **276** 1242
[28] Merkel S and Yagi T 2005 *Rev. Sci. Instrum.* **76** 46109-1
[29] Lin J F, Shu J, Mao H K, Hemley R J and Shen G 2003 *Rev. Sci. Instrum.* **74** 4732
[30] Singh A K, Mao H K, Shu J and Hemley R J 1998 *Phys. Rev. Lett.* **80** 2157
[31] Li L, Weidner D J, Chen J, Vaughan M T, Davis M and Durham W B 2004 *J. Appl. Phys.* **95** 8357
[32] Weidner D J, Li L, Davis M and Chen J 2004 *Geophys. Res. Lett.* **31** L06621